

Spin chain on a metallic surface: Dissipation-induced order versus Kondo entanglement

Bimla Danu¹, Matthias Vojta², Tarun Grover³, and Fakher F. Assaad¹


¹*Institut für Theoretische Physik und Astrophysik and Würzburg-Dresden Cluster of Excellence ct.qmat,*

Universität Würzburg, 97074 Würzburg, Germany

²*Institut für Theoretische Physik and Würzburg-Dresden Cluster of Excellence ct.qmat,*

Technische Universität Dresden, 01062 Dresden, Germany

³*Department of Physics, University of California at San Diego, La Jolla, California 92093, USA*

 (Received 18 April 2022; revised 8 August 2022; accepted 16 September 2022; published 4 October 2022)

We explore the physics of a spin-1/2 Heisenberg chain with Kondo interaction, J_k , to a two-dimensional electron gas. At weak J_k the problem maps onto a Heisenberg chain locally coupled to a dissipative Ohmic bath. At the decoupled fixed point, the dissipation is a marginally relevant perturbation and drives long-range antiferromagnetic order along the chain. In the dynamical spin structure factor we observe a quadratic low-energy dispersion akin to Landau-damped Goldstone modes. At large J_k Kondo screening dominates, and the spin correlations of the chain inherit the power law of the host metal, akin to a paramagnetic heavy Fermi liquid. In both phases we observe heavy bands near the Fermi energy in the composite-fermion spectral function. Our results, obtained from auxiliary-field quantum Monte Carlo simulations, provide a negative-sign-free realization of a quantum transition between an antiferromagnetic metal and a heavy-fermion metal. We discuss the relevance of our results in the context of scanning tunneling spectroscopy experiments of magnetic adatom chains on metallic surfaces.

DOI: [10.1103/PhysRevB.106.L161103](https://doi.org/10.1103/PhysRevB.106.L161103)

Introduction. A spin-1/2 antiferromagnetic chain embedded in a higher-dimensional metal, with Kondo coupling J_k between spins and electrons, represents an arena for rich physics. For two-dimensional metals, this relates to scanning tunneling microscopy (STM) experiments, with the ability to build and probe assemblies of magnetic adatoms on surfaces [1–5]. In higher dimensions, $\text{Yb}_2\text{Pt}_2\text{Pb}$ provides a realization of one-dimensional spin chains embedded in a three-dimensional metal [6,7]. Due to the dimensionality mismatch, such a system remains metallic even for a half-filled conduction band. It can host a variety of phases that include Kondo-breakdown or orbital-selective Mott states [8,9], heavy-fermion physics in which the magnetic spins, albeit subextensive, participate in the Luttinger volume, as well as non-Fermi-liquid states [10]. The understanding of quantum transitions between these states is of considerable interest both experimentally and theoretically.

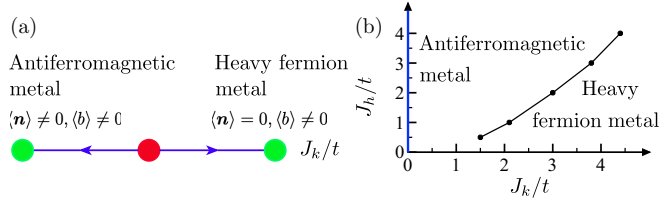
In this Letter we consider the above setup for two-dimensional electrons in the presence of a Fermi surface. In the limit of weak Kondo coupling, one can follow the Hertz-Millis approach [11,12] and perturbatively integrate out the fermions to arrive at an effective description of the spin chain locally coupled to an Ohmic bath [13–17]. As argued in Ref. [17], for an $\text{O}(3)$ quantum rotor model coupled to an Ohmic bath, the dissipation is marginally relevant and leads to long-range magnetic ordering along the chain. Hence, unlike in conventional heavy-fermion systems where Ruderman-Kittel-Kasuya-Yosida (RKKY) interactions directly drive magnetic ordering [18,19], here the ordering is stabilized

only by the dissipation. As the Kondo coupling increases, Kondo screening will compete with dissipation-induced ordering. In particular, in the strong-coupling limit it is expected that the spin-rotation symmetry will be restored in the chain, and the spin-spin correlations of the chain will inherit the power-law decay of the host metal. The physics of the Heisenberg spin chain on a metallic surface can hence be cast into the flow diagram of Fig. 1(a), where Kondo-singlet formation and dissipation-induced order compete.

Model and method. Our starting point is the Hamiltonian for a spin-1/2 chain on a metallic surface,

$$\hat{H} = -t \sum_{\langle i,j \rangle} (\hat{c}_i^\dagger \hat{c}_j + \text{H.c.}) + \frac{J_k}{2} \sum_{r=1}^L \hat{c}_r^\dagger \sigma \hat{c}_r \cdot \hat{S}_r + J_h \sum_{r=1}^L \hat{S}_r \cdot \hat{S}_{r+\Delta r}. \quad (1)$$

Here, the summation $\sum_{\langle i,j \rangle}$ runs over nearest neighbors of a square-lattice, $L \times L$, conducting substrate, t is the hopping matrix element, and $\hat{c}_i^\dagger = (\hat{c}_{i,\uparrow}^\dagger, \hat{c}_{i,\downarrow}^\dagger)$ is a spinor where $\hat{c}_{i,\uparrow(\downarrow)}^\dagger$ creates an electron at site i with z component of spin $1/2$ ($-1/2$). \hat{S}_r are spin-1/2 operators, and L is the length of the chain. We consider an array of adatoms at an interatomic spacing $\Delta r = (a, 0)$ with $a = 1$ and periodic boundary conditions are used along the spin chain as well as for the conduction electrons. Translation by $(a, 0)$ is a symmetry of the problem such that crystal momentum \mathbf{k} along the chain is conserved



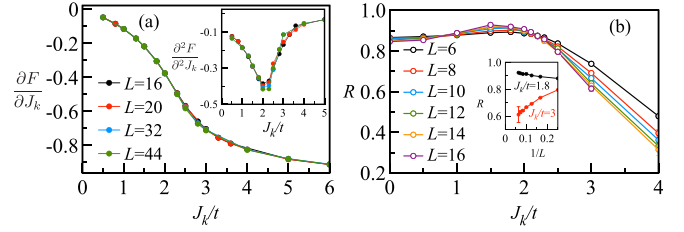
up to a reciprocal lattice vector. This model, including the Heisenberg exchange, is motivated by the STM work of Ref. [1].

In the absence of Kondo coupling and at $J_h \neq 0$, the local moments at low energies are described by a Luttinger liquid action $\mathcal{S}_{\text{chain}}$. Denoting the fluctuating antiferromagnetic (AFM) order parameter as \mathbf{n} , in this theory $\langle \mathbf{n}(\mathbf{r}, \tau) \cdot \mathbf{n}(\mathbf{0}, 0) \rangle \sim \sqrt{\log(r^2 + \tau^2)} / \sqrt{r^2 + \tau^2}$. Here $r = |\mathbf{r}|$. When $J_k \neq 0$, one may proceed by integrating out the conduction electrons and obtain an action up to second order in J_k as $\mathcal{S} = \mathcal{S}_{\text{chain}} + \mathcal{S}_{\text{diss}}(\mathbf{n})$, with

$$\mathcal{S}_{\text{diss}}(\mathbf{n}) = \frac{J_k^2}{8} \int d\tau d\tau' \sum_{\mathbf{r}, \mathbf{r}'} \mathbf{n}_r(\tau) \chi^0(\mathbf{r} - \mathbf{r}', \tau - \tau') \mathbf{n}_{r'}(\tau'), \quad (2)$$

where χ^0 is the antiferromagnetic spin susceptibility of the conduction electrons and $\mathcal{S}_{\text{chain}}$ the action of the spin chain. For generic, non-nested two-dimensional electrons at finite density, $\chi^0(\mathbf{r} = 0, \tau) \sim 1/\tau^2$, while $\chi^0(\mathbf{r}, \tau = 0) \sim 1/r^3$. Using power counting, one observes that while the long-range $1/r^3$ spatial decay of χ^0 is irrelevant at the $J_k = 0$ fixed point, the long-range $1/\tau^2$ decay in the time direction is not innocuous and at the leading order, corresponds to an dissipative Ohmic bath that is marginal in the renormalization-group sense. In fact, as argued in [17], such a dissipative coupling is a marginally relevant operator that triggers long-range order. To avoid the negative-sign problem, we employ a particle-hole-symmetric conduction band such that the Fermi surface is nested. As shown in the Supplemental Material [20], this leads to a multiplicative logarithmic correction to χ^0 : $\chi^0(\mathbf{0}, \tau) \sim \log^2(\tau)/\tau^2$. Therefore, at small J_k the logarithmic enhancement only increases the tendency for the system to become ordered due to dissipation. A particularity of the nested Fermi surface is a directional dependence of $\chi^0(\mathbf{r}, 0)$ [20]. For a chain along the $(a, 0)$ direction, $\chi^0(\mathbf{r}, 0) \sim 1/r^4$. At $J_k \gg J_h, t$ the local moments prefer to form local singlets with the conduction electrons, thereby resulting in a paramagnetic phase.

We simulate the Hamiltonian of Eq. (1) using the auxiliary-field quantum Monte Carlo (AFQMC) [21,22] implementa-



tion of the Algorithms for Lattice Fermions (ALF) [23,24] library. The model falls in the general category of spin-fermion Hamiltonians [25] that do not suffer from the sign problem. Our simulations are based on the finite-temperature grand-canonical AFQMC [26,27]. To reduce finite-size effects, we have included an orbital magnetic field of magnitude $B = \Phi_0/L^2$, where Φ_0 is the flux quantum [28].

AFQMC results. Given the above considerations, we anticipate an order-disorder transition as a function of J_k . To locate it, we consider $\frac{\partial F}{\partial J_k} = \frac{2}{3L} \sum_r \langle \hat{\sigma}_r^z \hat{\sigma}_r \cdot \hat{\mathbf{S}}_r \rangle$ as a function of J_k as well as $\frac{\partial^2 F}{\partial J_k^2}$ [Fig. 2(a) and inset]. As apparent, the data is consistent with a single transition at $J_k^c/t \simeq 2.1$ for $J_h/t = 1$. Next we consider the spin susceptibility,

$$\chi(\mathbf{k}, i\Omega_m) = \int_0^\beta d\tau \sum_r e^{i(\Omega_m \tau - \mathbf{k} \cdot \mathbf{r})} \langle \hat{S}_r^z(\tau) \hat{S}_0^z(0) \rangle, \quad (3)$$

from which we can define the correlation ratio,

$$R = 1 - \frac{\chi(\mathbf{Q} - \delta\mathbf{k}, 0)}{\chi(\mathbf{Q}, 0)}, \quad (4)$$

where $\mathbf{Q} = (\pi/a, 0)$ corresponds to the antiferromagnetic wave vector and $\delta\mathbf{k}$ to the smallest wave vector on the L -site chain. This correlation ratio scales to unity (zero) for ordered (disordered) states and at criticality is a renormalization-group-invariant quantity. Here, $R = f([J_k - J_k^c]L^{1/\nu}, L^z/\beta, L^{-\omega})$, where ν is the correlation length exponent, z is the dynamical exponent, and ω captures corrections to scaling. Figures 3(c) and 3(d) show that in the vicinity of the critical point, spatial correlations drop off as $1/r$, whereas

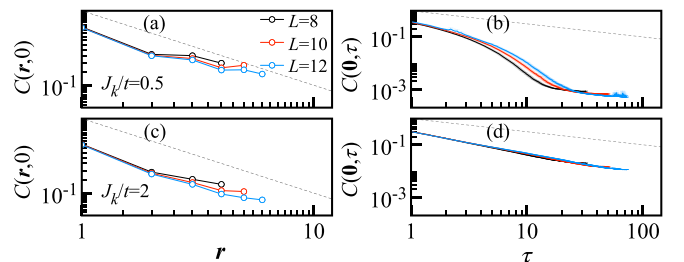


FIG. 3. Space and time correlation functions $C(\mathbf{r}, \tau)$ at $\beta t = L^2$ and $J_h/t = 1$. (a) $C(\mathbf{r}, 0)$ at $J_k/t = 0.5$. (b) $C(\mathbf{0}, \tau)$ at $J_k/t = 0.5$. (c) $C(\mathbf{r}, 0)$ at $J_k/t = 0.5$. (d) $C(\mathbf{0}, \tau)$ at $J_k/t = 2$. The dashed gray lines denote the $1/r$ [(a) and (c)] and $1/\sqrt{\tau}$ [(b) and (d)] power laws.

along the imaginary time, we observe a much slower $1/\sqrt{\tau}$ decay. This suggests a critical exponent $z \simeq 2$. With this in mind we can compute R , adopting a $\beta t = L^2$ scaling such that under the assumption of vanishing correlations to scaling, R should show a crossing point as a function of system size at J_k^c . As apparent from Fig. 2(b), R shows a crossing at $J_k^c/t \simeq 2.1$, thus providing a consistency check for our choice of the dynamical exponent. We now discuss the physics at weak, $J_k < J_k^c$, and strong, $J_k > J_k^c$, coupling.

For $J_k < J_k^c$, we expect dissipation-induced long-range AFM ordering. As discussed in [20], in this phase one can decompose the fluctuating AFM field \mathbf{n} as $\mathbf{n}(r, \tau) = (\boldsymbol{\sigma}(r, \tau), \sqrt{1 - \boldsymbol{\sigma}(r, \tau)^2})$, where the ordering is assumed along the \hat{z} direction. The low-energy action for the transverse fluctuations $\boldsymbol{\sigma}$ has dynamical exponent $z = 2$ and is given by $S_0(\boldsymbol{\sigma}) = \frac{\Gamma}{2} \int d\tau d\tau' dr \frac{\boldsymbol{\sigma}(r, \tau) \cdot \boldsymbol{\sigma}(r, \tau')}{(\tau - \tau')^2} + \frac{\rho_s}{2} \int d\tau dr [\partial_\tau \boldsymbol{\sigma}(r, \tau)]^2$. This implies that while the n^z correlations are long-ranged in both space and time, the correlations of $\boldsymbol{\sigma}$ are given as $\langle \boldsymbol{\sigma}(r, \tau) \cdot \boldsymbol{\sigma}(r, 0) \rangle \sim 1/\sqrt{\tau}$, while $\langle \boldsymbol{\sigma}(r, \tau) \cdot \boldsymbol{\sigma}(r, \tau) \rangle \sim 1/r$.

On the numerical front, at $J_k/t = 1.8 < J_k^c/t$, we observe a slight increase in the correlation ratio [Fig. 2(b) inset], thus hinting at the onset of long-range order, but as J_k decreases further, no sign of long-range order on our finite lattice sizes is apparent. To understand this apparent lack of ordering, we can switch off the Kondo screening and retain only local dissipation, corresponding to Eq. (2) with $\chi^0(r, \tau) \propto \delta_{r,0}/\tau^2$. For this bosonic model stochastic series approaches for retarded interactions [29,30] can be used to investigate this model with unprecedented precision [17]. It was shown in Ref. [17] that the marginally relevant nature of the Ohmic dissipation at the LL critical point requires lattice sizes $L \ll L_c \propto e^{\xi/J_k^c}$ to detect long-range order.

For $L \lesssim L_c$ one observes crossover phenomena characterized by a $1/r$ decay of the real-space spin-spin correlations and breakdown of Lorentz symmetry. Our understanding is that our data falls in this crossover regime and that for $r \ll L_c$ it can be accounted for by

$$C(r, \tau) \propto \begin{cases} \frac{1}{\sqrt{r^2 + \tau^{2/z}}} & \tau \ll \frac{1}{\Delta} \\ \frac{e^{-\Delta\tau}}{e^{r^2 + \Delta^{-2/z}}} & \tau \gg \frac{1}{\Delta} \end{cases} \quad (5)$$

on an L -site lattice. Here $C(r, \tau) = e^{i\mathbf{Q} \cdot \mathbf{r}} \langle \hat{S}_r^z(\tau) \hat{S}_0^z(0) \rangle$, and $\Delta \propto (\frac{2\pi}{L})^z$ corresponds to the finite-size gap. At $J_k/t = 0.5$, far from the critical point, Fig. 3 plots $C(r, 0)$ (a) as well as $C(0, \tau)$ (b). The real-space equal-time decay is consistent with a $1/r$ law. Along the imaginary time we observe crossover phenomena: While at short times, $\tau t \lesssim L$, the temporal decay is consistent with Eq. (5) at $z \simeq 1$ akin to the Heisenberg model, we observe at large τ a breakdown of Lorentz invariance, with $C(0, \tau)$ decaying substantially slower than $1/\tau$. In the infinite-size limit, we foresee that both the real-space and imaginary-time correlations will level off to show long-ranged correlations, albeit with a very small local moment.

The breakdown of Lorentz invariance is equally apparent in the data of Fig. 4. The ansatz of Eq. (5) leads a structure factor $S(\mathbf{Q}) = \frac{1}{\beta} \sum_{\Omega_m} \chi(\mathbf{Q}, i\Omega_m)$ that is independent of the dynamical exponent and as for the Heisenberg chain diverges as $\log(L)$. The size scaling in the crossover regime [Fig. 4(a)]

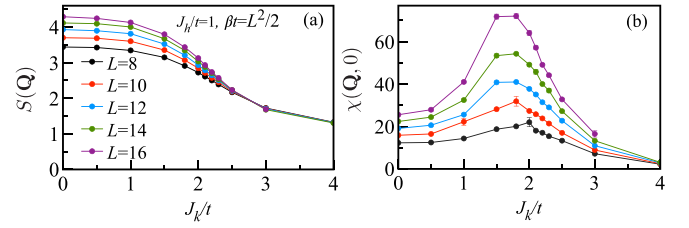


FIG. 4. (a) Static spin structure factor $S(\mathbf{Q})$ along the spin chain as a function of J_k/t for given L at $J_h/t = 1$ and $\beta t = L^2/2$. (b) Correspondingly, spin susceptibility $\chi(\mathbf{Q}, 0)$ as a function of J_k/t .

does not show marked differences from the Heisenberg limit. As noted in Ref. [17] and seen in Fig. 4(a), coupling to the bath reduces the magnitude of the equal-time spin correlations. On the other hand, the susceptibility, $\chi(\mathbf{Q}, 0)$, shows marked differences as a function of J_k . In Fig. 4(b) we consider the scaling $\beta t = L^2/2$. In the Heisenberg limit this leads to $\chi(\mathbf{Q}, 0) \propto L$, and a marked deviation from this law is observed in the crossover regime. For $z = 2$ akin to the critical point, $J_k^c/t \simeq 2.1$, the ansatz of Eq. (5) yields $\chi(\mathbf{Q}, 0) \propto L^2$. This scaling law is supported by the data, thus confirming $z \simeq 2$ at criticality.

At $J_k > J_k^c$ we are in a Kondo screened phase that can be understood within a large- N mean-field theory presented in Ref. [20]. In this phase, the spin-spin correlations inherit the asymptotic behavior of the conduction electrons and fall off as $1/r^4$ in space and as $1/\tau^2$ in imaginary time. In particular, Figs. S2 and S3 of Ref. [20] plot the space- and time-displaced correlation functions within the large- N approximation and confirm the above. The AFQMC data of Fig. 5 is consistent with this expectation.

Using the ALF [24] implementation of the maximum entropy method [31,32] we compute the dynamical spin structure factor $S(\mathbf{k}, \omega) = \frac{\text{Im}\chi(\mathbf{k}, \omega + i0^+)}{1 - e^{-\beta\omega}}$. Figure 6(a) plots this quantity for the Heisenberg model. The data shows the well-known two-spinon continuum [33–35]. At finite Kondo couplings [Figs. 6(b) and 6(c)], the two-spinon continuum is still apparent at elevated energies. However the low-energy bound shows a marked deviation from the linear dispersion and is very suggestive of a $\omega \propto k^2$ law. In fact, a field theory presented in Ref. [20] as well as a large- S calculation [17] of a Heisenberg chain locally coupled to an Ohmic bath confirms that dissipation stabilizes long-range order and that the lower bound of the dispersion relation follows an $\omega \propto k^2$

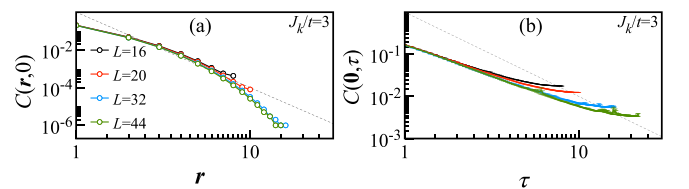


FIG. 5. Space and time correlation functions along the spin chain in the Kondo-screened phase at $J_h/t = 1$, $J_k/t = 3$, and $\beta t = L$. (a) $C(r, 0)$. The dashed gray line indicates a $1/r^4$ power law. (b) $C(0, \tau)$. The dashed gray line indicates a $1/\tau^2$ law. Both power laws in time and in space are observed in the large- N limit (see Ref. [20]).

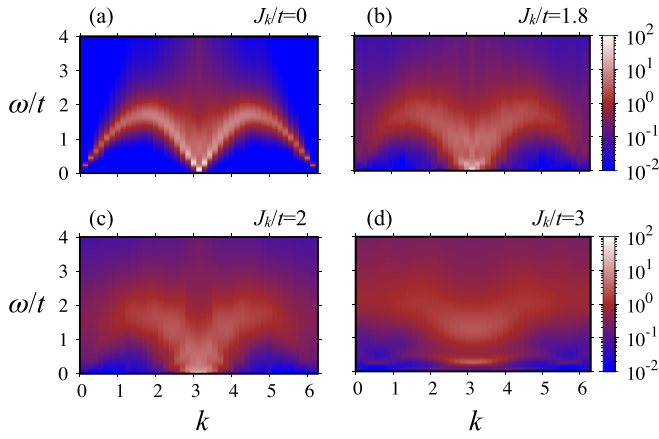


FIG. 6. $S(k, \omega)$ as a function of energy ω/t and momentum k along the spin chain at $\beta t = L = 44$ and $J_h/t = 1$.

law akin to Landau-damped Goldstone modes. Our dynamical data bears similarities with spinon binding as observed in KCuF_3 [36] and corresponds to a dimensional crossover [37]. In the present case, the elevated energy spectrum shows the two-spinon continuum, while the low energy corresponds to the spin-wave excitations of the Heisenberg chain coupled to an Ohmic bath [20]. Finally, in the Kondo-screened phase at $J_k/t = 3$, see Fig. 6(d), the low-lying spectral weight is depleted.

We now turn our attention to Kondo screening and heavy-fermion physics. Consider the composite-fermion operator $\hat{\psi}_{r,\sigma}^\dagger = 2 \sum_{\sigma'} \hat{c}_{r,\sigma'}^\dagger \sigma_{\sigma',\sigma} \cdot \hat{S}_r$ [38–40]. In the large- N limit this quantity picks up the Higgs condensate or hybridization matrix element [20], characteristic of Kondo screening [41]. Here we compute the spectral function $A_\psi(\mathbf{k}, \omega) = -\text{Im}G_\psi^{\text{ret}}(\mathbf{k}, \omega)$ with $G_\psi^{\text{ret}}(\mathbf{k}, \omega) = -i \int_0^\infty dt e^{i\omega t} \sum_\sigma \langle \{\hat{\psi}_{\mathbf{k},\sigma}(t), \hat{\psi}_{\mathbf{k},\sigma}^\dagger(0)\} \rangle$, representing the conduction-electron T matrix. Figures 7(a) and 7(b) show flat (i.e., heavy) bands in the vicinity of the Fermi energy, both below and above the critical point $J_k^c/t \simeq 2.1$. In Fig. 7(c) we plot $A_\psi(\omega) = \frac{1}{L} \sum_{\mathbf{k}} A_\psi(\mathbf{k}, \omega)$ as a function of temperature and J_k . To avoid analytical continuation, we use the relation $A_\psi(\omega = 0) \simeq (1/\pi)\beta G_\psi(\tau = \beta/2)$. Confirming the \mathbf{k} -dependent data, we see that this quantity never vanishes at low temperatures in both phases. Hence, the data supports the point of view that Kondo screening is active in the dissipation-induced ordered phase. It is interesting to note that the temperature dependence of $A_\psi(\omega = 0)$ differs in both phases. While it grows and saturates in the Kondo-screened phase, it shows a maximum in the ordered phase. Such a behavior can be understood in terms of the onset of ordering that opens a pseudogap in the spectral function, see Ref. [20]. $A_\psi(\omega = 0)$ is an important quantity since it provides a link to STM experiments. In fact, it corresponds to the zero-bias signal $dI/dV(V = 0)$ for tunneling processes between the tip and the substrate that involve intermediate excited states of the localized orbital. In the experiments described in Refs. [1,42] and modeled in Ref. [5], J_k can be tuned by changing the width of the Cu_2N islands between the Co adatoms and the $\text{Cu}(100)$ surface. Provided that the chains are long enough, our observation of distinct temperature behaviors of $A_\psi(\omega = 0)$ in

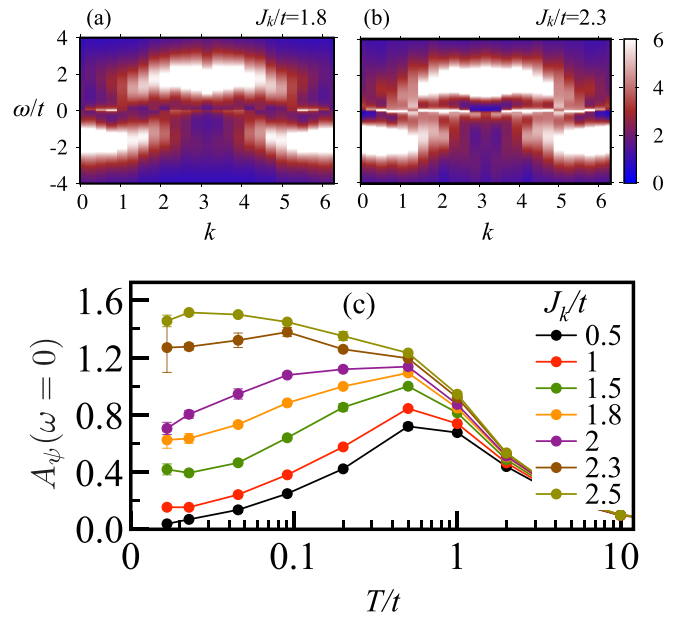


FIG. 7. Spectral function of the composite-fermion operator $A_\psi(k, \omega)$ on an $L = 24$ lattice at $\beta t = 48$ (a) in the ordered phase and (b) in the Kondo-screened phase. (c) Local zero-bias signal $A_\psi(\omega = 0)$ as a function of temperature T/t at $L = 44$ and for various values of J_k/t in the ordered and disordered phases.

the two phases provides a means to experimentally distinguish them.

Conclusions. The physics of the Heisenberg chain coupled to two-dimensional electrons can be understood by the competition between dissipation and Kondo screening. As the competition between the RKKY interaction and Kondo screening, the Kondo coupling triggers both effects but at different energy scales.

At weak coupling dissipation dominates, and the chain develops long-range antiferromagnetic order. Since the coupling to the Ohmic bath is marginally relevant [17], system sizes exceeding our achievable lattices are required to unambiguously detect the order. As a consequence, our data below the critical point are dominated by a crossover regime characterized by the absence of Lorentz invariance, as seen in Ref. [17]. In fact, the tendency towards ordering on small lattices can be enhanced by considering the XXZ (as opposed to Heisenberg) chain in its Luttinger-liquid phase. Here the transverse spin operator acquires a scaling dimension smaller than $1/2$ such that the coupling to the Ohmic bath becomes relevant. In Ref. [20] we have verified that the XXZ chain indeed leads to a stronger tendency towards ordering. At strong coupling, Kondo screening dominates, leading to a paramagnetic phase. Here, the spin-spin correlations inherit the power-law decay of the host metal. Aspects of this phase diagram have been put forward based on analytical considerations in Ref. [43].

The composite-fermion spectral function reveals a heavy band in both phases. Hence, in the ordered phase Kondo screening coexists with dissipation-induced ordering. In the disordered phase, the notion of heavy Fermi liquid can be made precise by invoking the Luttinger theorem that relates

the size of the Fermi surface to the count of its constituents. Since our model preserves translation invariance along the chain, it can be thought of as a one-dimensional model with a unit cell that contains L conduction electrons and single spin-1/2 local moment. With this formulation, one can now apply Oshikawa's proof of Luttinger theorem in the context of Kondo lattices [44] and show that the volume of the Fermi surface includes the local moments, assuming that the system is described by a Fermi liquid at low energies. An explicit calculation is presented in Ref. [20].

Our model provides a negative-sign-free realization of a Hertz-Millis-type transition between antiferromagnetic and paramagnetic heavy-fermion metals. In previous studies that capture aspects of Hertz-Millis-type physics [45], the electrons are effectively coupled to Ising spins such that Kondo effect and concomitant heavy-Fermi-liquid phase is not present. To avoid the negative-sign problem, we have to consider a particle-hole-symmetric conduction band with inherent nesting instabilities. Nevertheless, we expect that our broad conclusions, including the global structure of the phase diagram, hold for a generic two-dimensional Fermi surface. In the latter case, the spin-spin correlations of the host metal decay as $1/r^3$ and as $1/\tau^2$ in space and time, respectively. Since the $1/r^3$ decay is an irrelevant perturbation at the decoupled

fixed point, we expect dissipation-induced ordering to occur generically at small J_k . Remarkably, STM has the ability to build atomic rings on metallic surfaces. Therefore the two phases and the associated critical point can be probed with the existing STM technologies. Our numerical data suggests that the transition in Fig. 1 is characterized by a dynamical exponent $z \simeq 2$. A detailed understanding of the transition, both on the numerical and analytical fronts, remains for future work.

Acknowledgments. F.F.A. thanks D. Luitz and M. Weber for discussions on the dissipative Heisenberg chain. The authors gratefully acknowledge the Gauss Centre for Supercomputing e.V. [48] for providing computing time on the GCS Supercomputer SUPERMUC-NG at the Leibniz Supercomputing Centre [49]. The research has been supported by the Deutsche Forschungsgemeinschaft through Grant No. AS 120/14-1 (F.F.A.), the Würzburg-Dresden Cluster of Excellence on Complexity and Topology in Quantum Matter - ct.qmat (EXC 2147, Project ID No. 390858490) (F.F.A. and M.V.), and SFB 1143 (Project ID No. 247310070) (M.V.). T.G. is supported by the National Science Foundation under Grant No. DMR-1752417 and is an Alfred P. Sloan Research Fellow. F.F.A. and T.G. thank the BaCaTeC for partial financial support.

-
- [1] R. Toskovic, R. van den Berg, A. Spinelli, I. S. Eliens, B. van den Toorn, B. Bryant, J. S. Caux, and A. F. Otte, *Nat. Phys.* **12**, 656 (2016).
- [2] D. J. Choi, R. Robles, S. Yan, J. A. J. Burgess, S. Rolf-Pissarczyk, J. P. Gauryacq, N. Lorente, M. Ternes, and L. Sebastian, *Nano Lett.* **17**, 6203 (2017).
- [3] M. Moro-Lagares, R. Korytár, M. Piantek, R. Robles, N. Lorente, J. I. Pascual, M. R. Ibarra, and D. Serrate, *Nat. Commun.* **10**, 2211 (2019).
- [4] D.-J. Choi, N. Lorente, J. Wiebe, K. von Bergmann, A. F. Otte, and A. J. Heinrich, *Rev. Mod. Phys.* **91**, 041001 (2019).
- [5] B. Danu, F. F. Assaad, and F. Mila, *Phys. Rev. Lett.* **123**, 176601 (2019).
- [6] L. S. Wu, W. J. Gannon, I. A. Zaliznyak, A. M. Tsvelik, M. Brockmann, J.-S. Caux, M. S. Kim, Y. Qiu, J. R. D. Copley, G. Ehlers, A. Podlesnyak, and M. C. Aronson, *Science* **352**, 1206 (2016).
- [7] W. J. Gannon, I. A. Zaliznyak, L. S. Wu, A. E. Feiguin, A. M. Tsvelik, F. Demmel, Y. Qiu, J. R. D. Copley, M. S. Kim, and M. C. Aronson, *Nat. Commun.* **10**, 1123 (2019).
- [8] M. Vojta, *J. Low Temp. Phys.* **161**, 203 (2010).
- [9] B. Danu, M. Vojta, F. F. Assaad, and T. Grover, *Phys. Rev. Lett.* **125**, 206602 (2020).
- [10] L. Classen, I. Zaliznyak, and A. M. Tsvelik, *Phys. Rev. Lett.* **120**, 156404 (2018).
- [11] J. A. Hertz, *Phys. Rev. B* **14**, 1165 (1976).
- [12] A. J. Millis, *Phys. Rev. B* **48**, 7183 (1993).
- [13] P. Werner, M. Troyer, and S. Sachdev, *J. Phys. Soc. Jpn.* **74**, 67 (2005).
- [14] P. Werner, K. Völker, M. Troyer, and S. Chakravarty, *Phys. Rev. Lett.* **94**, 047201 (2005).
- [15] M. A. Cazalilla, F. Sols, and F. Guinea, *Phys. Rev. Lett.* **97**, 076401 (2006).
- [16] Z. Yan, L. Pollet, J. Lou, X. Wang, Y. Chen, and Z. Cai, *Phys. Rev. B* **97**, 035148 (2018).
- [17] M. Weber, D. J. Luitz, and F. F. Assaad, *Phys. Rev. Lett.* **129**, 056402 (2022).
- [18] M. A. Ruderman and C. Kittel, *Phys. Rev.* **96**, 99 (1954).
- [19] K. Yosida, *Phys. Rev.* **106**, 893 (1957).
- [20] See Supplemental Material at <http://link.aps.org/supplemental/10.1103/PhysRevB.106.L161103> for logarithmic correction to power-law decay, stability of AFM phase, mean-field calculation, Luttinger theorem, XXZ spin chain, and for other AFQMC results, which includes Refs. [46,47].
- [21] R. Blankenbecler, D. J. Scalapino, and R. L. Sugar, *Phys. Rev. D* **24**, 2278 (1981).
- [22] S. R. White, D. J. Scalapino, R. L. Sugar, E. Y. Loh, J. E. Gubernatis, and R. T. Scalettar, *Phys. Rev. B* **40**, 506 (1989).
- [23] M. Bercx, F. Goth, J. S. Hofmann, and F. F. Assaad, *SciPost Phys.* **3**, 013 (2017).
- [24] F. F. Assaad, M. Bercx, F. Goth, A. Götz, J. S. Hofmann, E. Huffman, Z. Liu, F. Parisen Toldin, J. S. E. Portela, and J. Schwab, *SciPost Phys. Codebases* **1** (2022).
- [25] T. Sato, F. F. Assaad, and T. Grover, *Phys. Rev. Lett.* **120**, 107201 (2018).
- [26] F. F. Assaad and H. G. Evertz, in *Computational Many-Particle Physics*, edited by H. Fehske, R. Schneider, and A. Weiße, Lecture Notes in Physics, Vol. 739 (Springer, Berlin, Heidelberg, 2008), pp. 277–356.
- [27] S. Capponi and F. F. Assaad, *Phys. Rev. B* **63**, 155114 (2001).
- [28] F. F. Assaad, *Phys. Rev. B* **65**, 115104 (2002).
- [29] M. Weber, F. F. Assaad, and M. Hohenadler, *Phys. Rev. Lett.* **119**, 097401 (2017).
- [30] M. Weber, *Phys. Rev. B* **105**, 165129 (2022).
- [31] A. W. Sandvik, *Phys. Rev. B* **57**, 10287 (1998).
- [32] K. S. D. Beach, [arXiv:cond-mat/0403055](https://arxiv.org/abs/cond-mat/0403055).

- [33] J. des Cloizeaux and J. J. Pearson, *Phys. Rev.* **128**, 2131 (1962).
- [34] G. Müller, H. Thomas, H. Beck, and J. C. Bonner, *Phys. Rev. B* **24**, 1429 (1981).
- [35] J.-S. Caux and J. M. Maillet, *Phys. Rev. Lett.* **95**, 077201 (2005).
- [36] B. Lake, D. A. Tennant, C. D. Frost, and S. E. Nagler, *Nat. Mater.* **4**, 329 (2005).
- [37] M. Raczkowski and F. F. Assaad, *Phys. Rev. B* **88**, 085120 (2013).
- [38] T. A. Costi, *Phys. Rev. Lett.* **85**, 1504 (2000).
- [39] L. Borda, L. Fritz, N. Andrei, and G. Zaránd, *Phys. Rev. B* **75**, 235112 (2007).
- [40] M. Raczkowski and F. F. Assaad, *Phys. Rev. Lett.* **122**, 097203 (2019).
- [41] B. Danu, Z. Liu, F. F. Assaad, and M. Raczkowski, *Phys. Rev. B* **104**, 155128 (2021).
- [42] A. Spinelli, M. Gerrits, R. Toskovic, B. Bryant, M. Ternes, and A. F. Otte, *Nat. Commun.* **6**, 10046 (2015).
- [43] A. M. Lobos, M. A. Cazalilla, and P. Chudzinski, *Phys. Rev. B* **86**, 035455 (2012).
- [44] M. Oshikawa, *Phys. Rev. Lett.* **84**, 3370 (2000).
- [45] Y. Schattner, S. Lederer, S. A. Kivelson, and E. Berg, *Phys. Rev. X* **6**, 031028 (2016).
- [46] H. Tsunetsugu, M. Sigrist, and K. Ueda, *Rev. Mod. Phys.* **69**, 809 (1997).
- [47] A. Luther and I. Peschel, *Phys. Rev. B* **12**, 3908 (1975).
- [48] www.gauss-centre.eu.
- [49] www.lrz.de.